

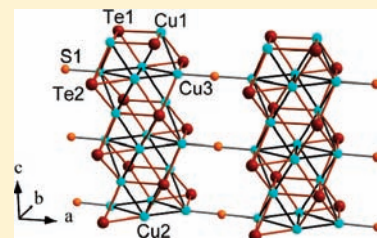
New Barium Copper Chalcogenides Synthesized Using Two Different Chalcogen Atoms: $\text{Ba}_2\text{Cu}_{6-x}\text{STe}_4$ and $\text{Ba}_2\text{Cu}_{6-x}\text{Se}_y\text{Te}_{5-y}$

Oottil Mayasree, Cheriyaedath Raj Sankar, Abdeljalil Assoud, and Holger Kleinke*

Department of Chemistry, University of Waterloo, Waterloo, Ontario, Canada N2L 3G1

Supporting Information

ABSTRACT: $\text{Ba}_2\text{Cu}_{6-x}\text{STe}_4$ and $\text{Ba}_2\text{Cu}_{6-x}\text{Se}_y\text{Te}_{5-y}$ were prepared from the elements in stoichiometric ratios at 1123 K, followed by slow cooling. These chalcogenides are isostructural, adopting the space group $Pbam$ ($Z = 2$), with lattice dimensions of $a = 9.6560(6)$ Å, $b = 14.0533(9)$ Å, $c = 4.3524(3)$ Å, and $V = 590.61(7)$ Å³ in the case of $\text{Ba}_2\text{Cu}_{5.53(3)}\text{STe}_4$. A significant phase width was observed in the case of $\text{Ba}_2\text{Cu}_{6-x}\text{Se}_y\text{Te}_{5-y}$ with at least $0.17(3) \leq x \leq 0.57(4)$ and $0.48(1) \leq y \leq 1.92(4)$. The presence of either S or Se in addition to Te appears to be required for the formation of these materials. In the structure of $\text{Ba}_2\text{Cu}_{6-x}\text{STe}_4$, Cu–Te chains running along the c axis are interconnected via bridging S atoms to infinite layers parallel to the a,c plane. These layers alternate with the Ba atoms along the b axis. All Cu sites exhibit deficiencies of up to 26%. Depending on y in $\text{Ba}_2\text{Cu}_{6-x}\text{Se}_y\text{Te}_{5-y}$, the bridging atom is either a Se atom or a Se/Te mixture when $y \leq 1$, and the Te atoms of the Cu–Te chains are partially replaced by Se when $y > 1$. All atoms are in their most common oxidation states: Ba^{2+} , Cu^+ , S^{2-} , Se^{2-} , and Te^{2-} . Without Cu deficiencies, these chalcogenides were computed to be small gap semiconductors; the Cu deficiencies lead to p -doped semiconducting properties, as experimentally observed on selected samples.



INTRODUCTION

Several tellurides of different stoichiometry in the Ba–Cu–Te system were studied with regard to their thermoelectric properties,^{1–4} including BaCu_2Te_2 ,⁵ $\text{A}_2\text{BaCu}_8\text{Te}_{10}$ ($A = \text{K, Rb, Cs}$),⁶ $\text{Ba}_3\text{Cu}_{14-x}\text{Te}_{12}$,⁷ and $\text{Ba}_{6.76}\text{Cu}_{2.42}\text{Te}_{14}$.⁸ In recent years, we reported the structures and properties of the first mixed Ba–Cu chalcogenides $\text{Ba}_3\text{Cu}_{17-x}\text{Se}_{11-y}\text{Te}_y$ ($2.0 \leq x \leq 2.6$; $2.4 \leq y \leq 3.3$)⁹ and $\text{Ba}_2\text{Cu}_{4-x}\text{Se}_y\text{Te}_{5-y}$ ($0.67 \leq x \leq 0.81$; $0.13 \leq y \leq 1.0$),¹⁰ both exhibiting mixed Se/Te occupancies and forming new structure types. While the former has no counterpart among the selenides or the tellurides, the telluride $\text{Ba}_2\text{Cu}_{4-x}\text{Te}_5$ adopts a type similar to $\text{Ba}_2\text{Cu}_{4-x}\text{Se}_y\text{Te}_{5-y}$, namely, with the same structure motifs but different interconnection of these motifs to the three-dimensional structure.

The strategy to use mixed anions, such as S/Te and Se/Te, for creation of new structures with mixed occupied chalcogen sites was demonstrated to be successful with the synthesis of $\text{Ta}_6\text{S}_{1+y}\text{Te}_{3-y}$ ($0 \leq y \leq 0.8$)¹¹ and $\text{Ta}_{15}\text{Si}_2\text{S}_y\text{Te}_{10-y}$ ($2.5 \leq y \leq 4$) and $\text{Ta}_{15}\text{Si}_2\text{Se}_y\text{Te}_{10-y}$ ($3 \leq y \leq 7$).¹² The general strategy dates back some 20 years, when new ternary Nb–Ta sulfides with differential fractional site occupancies on the cation sites were uncovered, namely, $\text{Nb}_{1.72}\text{Ta}_{3.28}\text{S}_2$,¹³ $\text{Nb}_{0.95}\text{Ta}_{1.05}\text{S}$,¹⁴ $\text{Nb}_{4.92}\text{Ta}_{6.08}\text{S}_4$,¹⁵ and $\text{Nb}_{6.74}\text{Ta}_{5.26}\text{S}_4$.¹⁶ That strategy became known as the DFSO concept^{17,18} and is neither limited to cationic elements of the same group or limited to chalcogenides, as evidenced by the germanide $\text{Ti}_{1.3}\text{Ta}_{9.7}\text{Ge}_8$ ¹⁹ and the pnictides $\text{Zr}_{7.5}\text{V}_{5.5}\text{Sb}_{10}$,²⁰ $\text{Hf}_3\text{Nb}_3\text{Ni}_3\text{P}_5$,²¹ and $\text{Hf}_{1.5}\text{Nb}_{1.5}\text{As}$.²² The concept was expanded by creating mixed anionic sites, like for Si and Sb in $\text{Ti}_5\text{Si}_{1.3}\text{Sb}_{1.7}$ ²³ and Sb and Se in $\text{Ti}_5\text{Sb}_{2.2}\text{Se}_{0.8}$.²⁴ Here, a new example is presented, where up to two of the three chalcogen

sites may be mixed occupied in the case of the selenide–telluride, $\text{Ba}_2\text{Cu}_{6-x}\text{Se}_y\text{Te}_{5-y}$, depending on the Se/Te ratio, while neither a phase range nor a mixed S/Te occupancy was detected within the experimental limits in the case of the isostructural sulfide–telluride, $\text{Ba}_2\text{Cu}_{6-x}\text{STe}_4$.

EXPERIMENTAL SECTION

Syntheses and Analyses. The reactions started from the elements, kept in an argon-filled glovebox (Ba pieces, 99% nominal purity, Sigma Aldrich; Cu powder, 99.9%, Alfa Aesar; S powder, 99.999%, Alfa Aesar; Se powder, 99.999%, Sigma Aldrich; Te powder, 99.8%, Sigma Aldrich). The new sulfide–telluride $\text{Ba}_2\text{Cu}_{5.5}\text{STe}_4$ was first obtained in an attempt to prepare a compound of the nominal composition “BaCuSTe” while trying to investigate the existence of nonclassical bonding in chalcogenides, as, for example, occurring in the linear Se_3^{4-} unit of $\text{Ba}_2\text{Ag}_4\text{Se}_5$.²⁵ Similar Se_3^{4-} units occurring in $\text{Rb}_{12}\text{Nb}_6\text{Se}_{35}$ ²⁶ are not quite linear, with bond angles of 163° and 164°.

The respective elements were loaded into a silica tube in the argon-filled glovebox followed by sealing the tube under vacuum. The fused tube was heated to 1073 K within 32 h and kept at that temperature for 48 h and then cooled down to 673 K at the rate of 1 K per hour, followed by switching off the furnace. A suitable single crystal was picked from the sample for single-crystal X-ray diffraction. Solving the structure by single-crystal X-ray determination proved the compound to be of a new structure type of the refined formula $\text{Ba}_2\text{Cu}_{6-x}\text{STe}_4$ with $x = 0.47(3)$, as explained in the succeeding section.

Received: February 7, 2011

Published: April 21, 2011

Table 1. Crystallographic Details of Ba₂Cu_{6-x}STe₄ and Ba₂Cu_{6-x}Se_yTe_{5-y}

refined formula	Ba ₂ Cu _{5.53(3)} STe ₄	Ba ₂ Cu _{5.43(4)} Se _{1.92(4)} Te _{3.08}	Ba ₂ Cu _{5.64(3)} Se _{1.10(1)} Te _{3.90}	Ba ₂ Cu _{5.83(3)} Se _{0.48(1)} Te _{4.52}
CSD-no.	422 906	422 907	422 905	422 908
fw [g/mol]	1168.83	1164.31	1217.78	1259.77
T of measurement [K]	296(2)	296(2)	296(2)	296(2)
λ [Å]	0.71073	0.71073	0.71073	0.71073
space group	<i>Pbam</i>	<i>Pbam</i>	<i>Pbam</i>	<i>Pbam</i>
a [Å]	9.6560(6)	9.638(2)	9.7048(6)	9.7728(9)
b [Å]	14.0533(9)	14.063(2)	14.1853(9)	14.372(1)
c [Å]	4.3524(3)	4.3714(7)	4.3840(3)	4.4125(4)
V [Å ³]	590.61(7)	592.5(2)	603.53(7)	619.8(1)
Z	2	2	2	2
μ [mm ⁻¹]	26.12	29.36	28.65	27.83
ρ _{calcd} [g/cm ³]	6.57	6.53	6.70	6.75
total, independent, observed reflections (R _{int})	4292, 955, 907 (0.030)	4295, 956, 887 (0.021)	4345, 978, 974 (0.018)	9068, 1011, 916 (0.15)
R(F _o)/R _w (F _o ²) all	0.026/0.060	0.034/0.067	0.021/0.044	0.035/0.079
R(F _o)/R _w (F _o ²) obs	0.025/0.058	0.031/0.065	0.020/0.043	0.032/0.077

The synthesis of a phase pure sample was attempted within a glassy carbon crucible embedded in a fused silica tube starting from the 2:5.5:1:4 (Ba:Cu:S:Te) ratio. This mixture was heated to 1173 K within 48 h, kept at 1173 K for 48 h, and cooled down with 1 K per minute. Thereafter the product was ground and analyzed using a powder X-ray diffractometer with a position-sensitive detector (Inel) employing Cu Kα₁ radiation. The powder XRD pattern of the sample indicated that the sample is single phase when compared with the pattern simulated from the refined crystal data.

Attempts were made to synthesize isostructural compounds with varying chalcogen atoms and with different coinage metals. However, substitution of Cu by Ag or Au was not possible, at least not with the above-mentioned or similar conditions. Reactions of nominal compositions “Ba₂Cu_{5.5}Se₄”, “Ba₂Cu_{5.5}S₅”, “Ba₂Cu_{5.5}Se₅”, and “Ba₂Cu_{5.5}Te₅” gave XRD patterns with BaCu₂S₂, BaCu₂Se₂,²⁷ and BaCu₂Te₂⁵ as major phases under the same reaction conditions. A reaction with Se substituting the S atom of Ba₂Cu_{5.5}STe₄ was successful. The single-crystal X-ray data of this compound yielded a refined formula of Ba₂Cu_{5.64(3)}Se_{1.10(1)}Te_{3.90}, and no side products were identified in its powder XRD pattern.

Phase range studies on Ba₂Cu_{6-x}S_yTe_{5-y} and Ba₂Cu_{6-x}Se_yTe_{5-y} were carried out by varying *y*, with *x* being between 0.5 and 0. No evidence for a significant phase range was found in the case of the sulfide–telluride. On the other hand, phase pure samples were obtained in the case of the selenide–telluride with 0.5 ≤ *y* ≤ 2. Single-crystal studies were then performed on selected crystals of both ends of this phase range, yielding refined Se contents of *y* = 0.48(1) and 1.92(4), respectively.

To check for homogeneity and the absence of unwanted heteroelements, the samples of nominal composition Ba₂Cu_{5.5}STe₄ and Ba₂Cu_{5.5}SeTe₄ were analyzed via energy-dispersive analysis of X-rays using an electron microscope (LEO 1530) with an additional EDX device (EDAX Pegasus 1200). No heteroelements were detected, and the Ba:Cu:S/Se:Te ratios were determined to be 15.5:44.9:8.1:31.5 atom % for the sulfide–telluride and 15.9:45.5:10.2:28.3 for the selenide–telluride, as averaged over several crystals. From crystal to crystal, the numbers varied within ±2 atom %. These numbers compare well with the ones calculated from the starting ratio (16.0:44.0:8.0:32.0).

The melting points of these materials were determined via differential scanning calorimetry (DSC) experiments under a flow of argon with the Netzsch STA 409PC Luxx.^{28,29} Melting points of 1063 and 1051 K were observed for Ba₂Cu_{5.5}STe₄ and Ba₂Cu_{5.5}SeTe₄, respectively.

Structure Determination. A black, plate-like single crystal of the nominal composition “BaCuSTe” was selected for structure determination,

which was performed with a Bruker Smart APEX CCD diffractometer with graphite-monochromatized Mo Kα₁ radiation via ω scans of 0.3° in two groups of 600 frames at φ = 0° and 90°. Each frame was exposed for 60 s to the radiation. The data were corrected for Lorentz and polarization effects, followed by an absorption correction based on fitting a function to the empirical transmission surface as sampled by multiple equivalent measurements using SADABS incorporated into the package SAINT within the APEX2 software package.³⁰

Unit cell parameters indicated orthorhombic symmetry. The structure was refined using the SHELXTL program.³¹ The systematic absences restricted the possible space groups to *Pba2* and *Pbam*. Using “direct methods” in the space group *Pbam* yielded a total of seven atomic sites, one Ba, three Cu, one S (called S1), and two Te atoms (Te1, Te2). The occupancy factors of the Cu sites were further refined, since refinement with full occupancies yielded large anisotropic displacement parameters in the case of all three Cu sites, most notably so for Cu2, thereby yielding deficiencies of 2% (Cu1), 20% (Cu2), and 1% (Cu3), and an R1 value of 0.026, compared to 0.036 for refinement with fully occupied Cu sites (all data). The Cu2 atom showed an elongated U₂₂ parameter, approximately three times larger than the average of the U₁₁ and U₃₃. Tentatively introducing split sites to Cu2 failed to improve the anisotropic displacement parameters. In addition, a tentative refinement in *Pba2* revealed neither an improvement in the refinement quality nor a partial ordering of the deficiencies. Moreover, we also refined all three chalcogen sites as mixed S/Te sites but found no significant deviation from the 100% S occupancy of S1 and 100% Te occupancy of both Te1 and Te2. Thus, refinement in *Pbam* without any split sites or S/Te mixed occupancies was considered as final. Lastly, all atomic positions were standardized with the help of the TIDY program within the PLATON package.³²

The data on three selenide–telluride crystals with different Se/Te ratios were collected and corrected via the same procedure, and its structure refinements commenced from the last refinement of the sulfide–telluride. In addition to refining the occupancies of the Cu sites, which yielded decreasing Cu deficiencies with increasing Te content, refining the occupancies of the Se and Te sites resulted in significant improvements of the R values as well as significant mixed occupancies on 1–2 of the three chalcogen sites. The refined formulas turned out to be Ba₂Cu_{5.43(4)}Se_{1.92(4)}Te_{3.08} (from a sample of nominal composition “Ba₂Cu_{5.5}Se₂Te₃”), Ba₂Cu_{5.64(3)}Se_{1.10(1)}Te_{3.90} (from “Ba₂Cu_{5.5}SeTe₄”), and Ba₂Cu_{5.83(3)}Se_{0.48(1)}Te_{4.52} (from “Ba₂Cu_{5.5}Se_{0.5}Te_{4.5}”). Crystallographic data of the four single-crystal refinements are summarized in Table 1, and the atomic parameters including the occupancy factors of the sulfide–telluride are listed in Table 2. The occupancy factors of

$\text{Ba}_2\text{Cu}_{6-x}\text{Se}_y\text{Te}_{5-y}$ are compared in Table 3. Further details of the crystal structure investigation can be obtained from the Fachinformationszentrum Karlsruhe, 76344 Eggenstein-Leopoldshafen, Germany, (fax (49) 7247-808-666; e-mail crysdata@fiz-karlsruhe.de) on quoting the various depository numbers (CSD 422905–422908, see Table 1).

Calculation of the Electronic Structure. We carried out LMTO (linear muffin tin orbitals) calculations with the atomic spheres approximation (ASA)^{33,34} to obtain the electronic structures of $\text{Ba}_2\text{Cu}_{5.5}\text{STe}_4$ and $\text{Ba}_2\text{Cu}_{5.6}\text{Se}_{1.1}\text{Te}_{3.9}$. Therein, density functional theory is applied with the local density approximation (LDA) to treat exchange and correlation effects.³⁵ The following wave functions were used: for Ba 6s, 6p (downfolded³⁶), 5d, and 4f; for Cu 4s, 4p, and 3d; for S 3s, 3p, and 3d (downfolded); for Se 4s, 4p, and 4d (downfolded); and for Te 5s, 5p, 5d, and 4f (the latter two downfolded). In both cases, all three Cu sites were considered as fully occupied and in the case of the selenide–telluride the Te2 site, refined to be mixed occupied with 5% Se and 95% Te, was considered as occupied solely by Te atoms. The formulas of these models are thus $\text{Ba}_2\text{Cu}_6\text{STe}_4$ and $\text{Ba}_2\text{Cu}_6\text{SeTe}_4$. Four hundred fifty five *k* points of the irreducible wedge of the first Brillouin zone were chosen via the improved tetrahedron method³⁷ for the calculations.

Table 2. Atomic Coordinates, Equivalent Isotropic Displacement Parameters, and Occupancy Factors of $\text{Ba}_2\text{Cu}_{5.5}\text{STe}_4$

atom	site	<i>x</i>	<i>y</i>	<i>z</i>	$U_{\text{eq}}/\text{\AA}^2$	occ.
Ba1	4h	0.02299(4)	0.16049(3)	1/2	0.0141(1)	1
Cu1	4h	0.3870(1)	0.09260(7)	1/2	0.0232(3)	0.978(5)
Cu2	4g	0.0274(1)	0.4099(1)	0	0.0356(5)	0.799(5)
Cu3	4g	0.2462(1)	0.00998(7)	0	0.0225(3)	0.987(4)
S1	2a	0	0	0	0.0131(4)	1
Te1	4h	0.17439(4)	0.40777(3)	1/2	0.0148(1)	1
Te2	4g	0.30983(4)	0.19610(3)	0	0.0131(1)	1

Table 3. Occupancy Factors of $\text{Ba}_2\text{Cu}_{6-x}\text{Se}_y\text{Te}_{5-y}$

atom	$\text{Ba}_2\text{Cu}_{5.4}\text{Se}_{1.9}\text{Te}_{3.1}$	$\text{Ba}_2\text{Cu}_{5.6}\text{Se}_{1.1}\text{Te}_{3.9}$	$\text{Ba}_2\text{Cu}_{5.8}\text{Se}_{0.5}\text{Te}_{4.5}$
Ba1	1	1	1
Cu1	0.870(7)	0.960(4)	0.980(5)
Cu2	0.864(7)	0.866(5)	0.936(5)
Cu3	0.979(6)	0.993(4)	0.997(5)
Se1	1	1	0.48(1) Se, 0.52 Te
Te1	0.15(1) Se, 0.85 Te	1	1
Te2	0.31(1) Se, 0.69 Te	0.048(7) Se, 0.952 Te	1

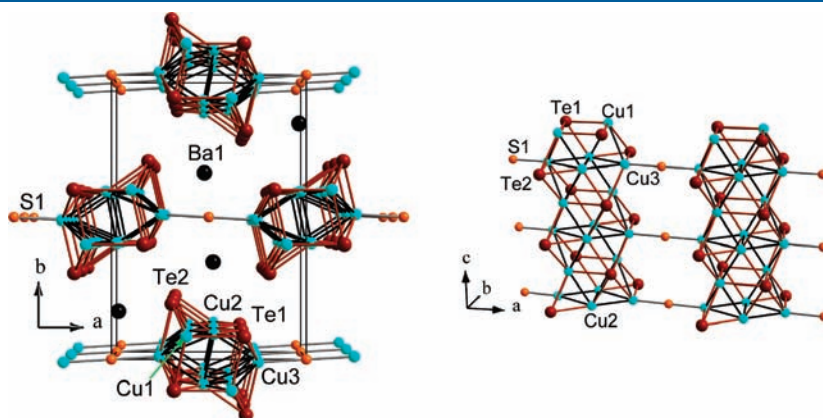


Figure 1. (Left) Crystal structure of $\text{Ba}_2\text{Cu}_{6-x}\text{STe}_4$. (Right) One $\text{Cu}_{6-x}\text{STe}_4$ layer. Ba–S and Ba–Te bonds are omitted for clarity.

Physical Property Measurements. Physical properties were determined on sintered cold-pressed pellets of nominal compositions $\text{Ba}_2\text{Cu}_{5.53}\text{STe}_4$ and $\text{Ba}_2\text{Cu}_{5.53}\text{SeTe}_4$. Bar-shaped pellets of dimensions $13 \times 2 \times 2$ mm, prepared under a pressure of 700 MPa, were used for simultaneous measurements of the Seebeck coefficient and electrical conductivity utilizing the ULVAC-RIKO ZEM-3 between 300 and 573 K. XRD measurements performed after the property measurements showed no signs of decomposition.

RESULTS AND DISCUSSION

Crystal Structures. The two new quaternary chalcogenides, $\text{Ba}_2\text{Cu}_{6-x}\text{STe}_4$ and $\text{Ba}_2\text{Cu}_{6-x}\text{Se}_{1.1}\text{Te}_{3.9}$, are isostructural, crystallizing in the orthorhombic crystal system with space group *Pbam*. The structure is composed of covalently bonded puckered

Table 4. Selected Interatomic Distances [Angstroms] of $\text{Ba}_2\text{Cu}_{6-x}\text{Q}_5$

interaction	$\text{Ba}_2\text{Cu}_{5.5}\text{-STe}_4$	$\text{Ba}_2\text{Cu}_{5.4}\text{-Se}_{1.9}\text{Te}_{3.1}$	$\text{Ba}_2\text{Cu}_{5.6}\text{-Se}_{1.1}\text{Te}_{3.9}$	$\text{Ba}_2\text{Cu}_{5.8}\text{-Se}_{0.5}\text{Te}_{4.5}$
Ba1–S1/Se1 $\times 2$	3.1420(3)	3.2275(6)	3.2270(3)	3.3105(4)
Ba1–Te1	3.5001(6)	3.545(1)	3.5608(6)	3.6293(7)
Ba1–Te1	3.7700(6)	3.693(1)	3.7448(7)	3.7367(8)
Ba1–Te2 $\times 2$	3.5577(5)	3.5357(9)	3.5622(5)	3.5741(5)
Ba1–Te2 $\times 2$	3.6103(5)	3.557(8)	3.5883(4)	3.5829(5)
Cu1–Te1	2.664(1)	2.648(2)	2.673(1)	2.688(1)
Cu1–Te1	2.775(1)	2.794(2)	2.796(1)	2.809(1)
Cu1–Te2 $\times 2$	2.7216(7)	2.732(1)	2.747(6)	2.7746(8)
Cu1–Cu2 $\times 2$	2.5641(9)	2.568(1)	2.5768(8)	2.5970(8)
Cu1–Cu3 $\times 2$	2.8163(9)	2.750(1)	2.7692(8)	2.752(1)
Cu2–Te1 $\times 2$	2.5983(8)	2.621(1)	2.6236(6)	2.6345(6)
Cu2–Te2	2.576(1)	2.535(2)	2.574(1)	2.599(1)
Cu2–Cu1 $\times 2$	2.5641(9)	2.568(1)	2.5768(8)	2.5970(8)
Cu2–Cu2	2.587(4)	2.677(3)	2.661(2)	2.715(3)
Cu2–Cu3	2.599(2)	2.576(2)	2.583(1)	2.583(2)
Cu2–Cu3	2.939(2)	2.825(2)	2.842(1)	2.809(2)
Cu3–S1/Se1	2.3818(9)	2.487(1)	2.4997(9)	2.575(1)
Cu3–Te1 $\times 2$	2.7179(7)	2.709(1)	2.7248(6)	2.7452(7)
Cu3–Te2	2.687(1)	2.635(2)	2.663(1)	2.663(1)
Cu3–Cu2	2.599(2)	2.574(2)	2.583(1)	2.583(2)
Cu3–Cu2	2.939(2)	2.825(2)	2.842(1)	2.809(2)
Cu3–Cu1 $\times 2$	2.8163(9)	2.750(1)	2.7692(8)	2.752(1)

Cu–Q layers (Q = S, Se, Te) stacked along the *b* axis that sandwich the Ba²⁺ cations (left part of Figure 1). The Ba atoms are 8-fold coordinated by two S1, two Te1, and four Te2 atoms in Ba₂Cu_{6–x}STe₄. Because of the absence of bonds between the chalcogen atoms, we can assign the 2– oxidation state to S, Se, and Te. With Ba²⁺, the Cu atoms would be all 1+ if all Cu sites were filled, as in “(Ba²⁺)₂(Cu⁺)₆S^{2–}(Te^{2–})₄”.

The layers of Ba₂Cu_{6–x}STe₄ consist of Cu–Te chains running along the *c* axis, interconnected via interchain S1 atoms with Cu3–S1 distances of 2.38 Å (right part of Figure 1). The Cu3–S1–Cu3 bridge is perfectly linear. Cu1 is bonded to two Te1 atoms at distances of 2.66 and 2.78 Å and two Te2 atoms at 2.72 Å (Table 4). Similarly, Cu3 is coordinated by two Te1, S1, and one Te2 atoms with distances of 2.72, 2.38, and 2.69 Å, respectively. On the other hand, Cu2 occurs in an almost planar CuTe₃ units, comparable to the CuTe₃ unit in Ba₃Cu_{14–x}Te₁₂⁷ and CuSe₃ in Ba₃Cu₂Sn₃Se₁₀,³⁸ which extend along the *c* axis via common Te1 atoms. The Cu2–Te1 (2×) and Cu2–Te2 distances of 2.60 and 2.58 Å are inconspicuous, being slightly larger than the sum of Pauling’s single-bond radii,³⁹ $r_{\text{Cu}} + r_{\text{Te}} = 1.18 + 1.37 = 2.55$ Å, while being shorter than the Cu–Te bonds of the 4-fold coordinated Cu atoms.

Numerous Cu–Cu contacts between 2.56 and 2.94 Å are present in the Cu–Te chains of Ba₂Cu_{6–x}STe₄, giving rise to

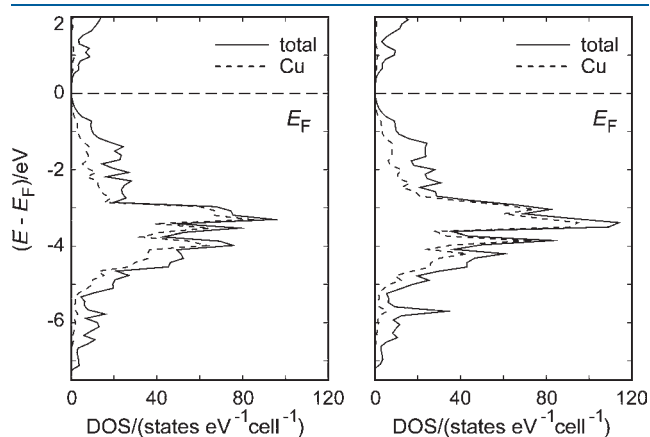


Figure 2. Densities of states (DOS) of Ba₂Cu₆STe₄ (left) and Ba₂Cu₆SeTe₄ (right). The dashed horizontal lines denote the Fermi level, E_F .

one-dimensionally extended Cu–Cu interactions. Similar Cu–Cu distances occur regularly in Cu⁺ chalcogenides,⁴⁰ including Ba₃Cu_{14–x}Te₁₂,⁷ Ba₃Cu_{17–x}Se_{11–y}Te_y,⁹ and Ba₂Cu_{4–x}Se_yTe_{5–y}.¹⁰ Theoretical investigations have shown that their bonding character is a consequence of hybridization effects.^{41–43}

In Ba₂Cu_{5.6}Se_{1.1}Te_{3.9}, Se atoms are connecting the topologically equivalent Cu–Te chains, which include small amounts of Se, namely, 5% on the Te2 site. Using more Se leads to mixed occupancies of both the Te1 and the Te2 sites, e.g., 15% and 31% Se, respectively, in the case of Ba₂Cu_{5.4}Se_{1.9}Te_{3.1}. On the other hand, using more Te leads to incorporation of Te on the “Se1” site that interconnects the Cu–Te chains. As a consequence, the Cu3–“Se1” distance increases from 2.50 to 2.58 Å, when “Se1” is occupied by 48% Se and 52% Te. No such mixed occupancies were detected in the case of the sulfide–telluride, likely because an S atom is much smaller than a Te atom, while the size difference between Se and Te is less pronounced ($r_{\text{S}} = 1.04$ Å, $r_{\text{Te}} = 1.37$ Å).

That no mixed S/Te occupancies were identified in the structure of Ba₂Cu_{6–x}STe₄ has its precedence in the structure of Zr₆STe₂.⁴⁴ Such mixed occupancies are possible, however, as is the case in Ta₆S_{1+x}Te_{3–x}¹¹ (with up to 4% S on Te sites and 7% Te on S sites) and Ta₁₅Si₂S_xTe_{10–x}¹² (with one pure S site and four mixed S/Te sites).

The special character of the S1/“Se1” position becomes evident from its short distances to the neighboring Cu atoms of <2.5 Å, which would be too short for Cu–Te distances. The preference of Se for Te2 over Te1 can also be related to the different bond distances; both Te1 and Te2 are coordinated by eight atoms, namely, Te1 by two Ba and six Cu and Te2 by four Ba and four Cu atoms. In the structure of Ba₂Cu_{5.8}Se_{0.5}Te_{4.5}, where these two sites are solely occupied by Te, the averaged Te2–Ba and Te2–Cu distances are both shorter than its Te1 counterparts: the Te2–Ba average of 3.58 Å is much shorter than Te1–Ba (3.65 Å), while the differences between the averaged Te–Cu bonds are less significant (2.68 vs 2.69 Å).

Electronic Structures and Physical Properties. The densities of states, DOS, of Ba₂Cu₆STe₄ and Ba₂Cu₆SeTe₄ are comparable, both exhibiting a very small band gap < 0.1 eV at the Fermi level (Figure 2). The valence bands are dominated by the 3d orbitals of the Cu⁺ atoms.

Noting that the experimentally obtained materials were all deficient in Cu, *p*-doped semiconducting properties are to be

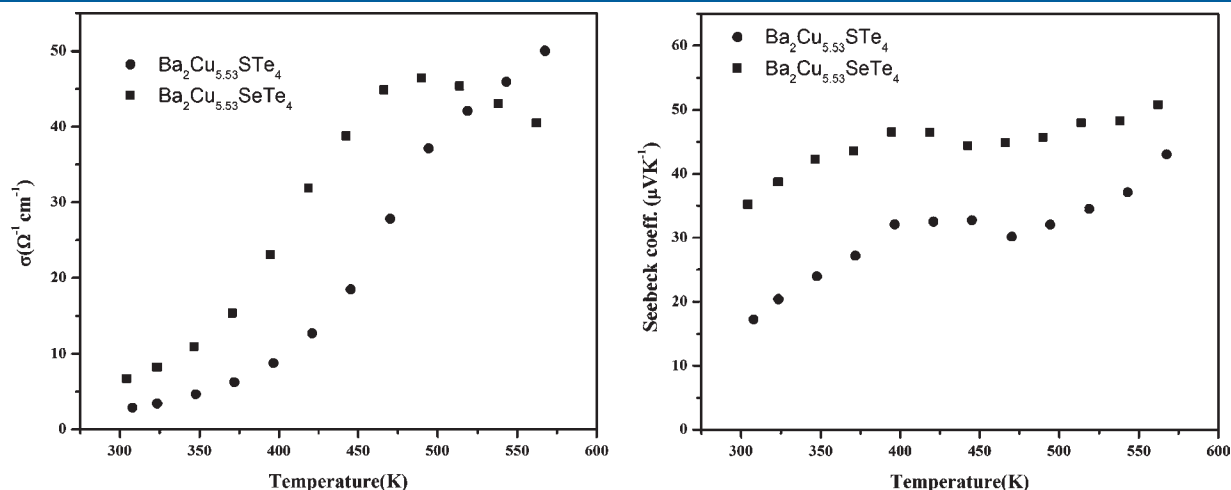


Figure 3. Electrical conductivity (left) and Seebeck coefficient (right) of Ba₂Cu_{5.53}STe₄ and Ba₂Cu_{5.53}SeTe₄.

expected. Confirming this expectation, the electrical conductivity, σ , of both $\text{Ba}_2\text{Cu}_{5.5}\text{STe}_4$ and $\text{Ba}_2\text{Cu}_{5.5}\text{SeTe}_4$ increases almost exponentially with increasing temperature to 450 K, e.g., from $7 \Omega^{-1} \text{cm}^{-1}$ at 305 K to $39 \Omega^{-1} \text{cm}^{-1}$ at 440 K in the case of the slightly higher conductive selenide–telluride, at which point the curve begins to flatten, reaches a maximum of $46 \Omega^{-1} \text{cm}^{-1}$ at 490 K, and then decreases to $40 \Omega^{-1} \text{cm}^{-1}$ at 560 K (left part of Figure 3). Similarly, the conductivity curve of the sulfide–telluride begins to flatten around 500 K. One reason for this effect could be an exhaustion of the thermally activated charge carriers, and the decrease in σ is caused by the then dominating negative temperature dependence of the carrier mobility.

Finally, the small values of the Seebeck coefficient, S (between $+15 \mu\text{V K}^{-1}$ at 300 K and $+35 \mu\text{V K}^{-1}$ at 573 K for the sulfide–telluride, with higher values from $+35$ to $+50 \mu\text{V K}^{-1}$ for the selenide–telluride), are typical for doped materials with very small band gaps, and the positive sign of the Seebeck coefficient confirms the p -doping (right part of Figure 3). The slight decrease after 400 K could be a sign of an increase in charge carrier concentration, n , by thermal activation, which coincides with the steepest part of the conductivity curve. When σ begins to flatten/decrease, indicative of a smaller increase in n , S increases again.

The fact that neither the conductivity nor the Seebeck coefficient are high enough for the thermoelectric energy conversion indicates that (further) doping will not be able to produce good thermoelectric properties. Increasing the carrier concentration typically increases σ and decreases S , while decreasing it would decrease σ and increase S .

CONCLUSIONS

With $\text{Ba}_2\text{Cu}_{6-x}\text{STe}_4$ and $\text{Ba}_2\text{Cu}_{6-x}\text{Se}_y\text{Te}_{5-y}$, two new mixed chalcogenides were synthesized and characterized, wherein all elements are in their most common oxidation states (Ba^{2+} , Cu^+ , S^{2-} , Se^{2-} , Te^{2-}). These chalcogenides adopt a hitherto unprecedented structure type. No mixed occupancies were detected for the sulfide–telluride, while a significant phase width exists in the case of $\text{Ba}_2\text{Cu}_{6-x}\text{Se}_y\text{Te}_{5-y}$, with $0.17(3) \leq x \leq 0.57(4)$ and $0.48(1) \leq y \leq 1.92(4)$. Of the three chalcogen sites, one is S and two are Te positions in $\text{Ba}_2\text{Cu}_{6-x}\text{STe}_4$, while depending on y , up to two sites may be mixed occupied in $\text{Ba}_2\text{Cu}_{6-x}\text{Se}_y\text{Te}_{5-y}$.

The structure of $\text{Ba}_2\text{Cu}_{6-x}\text{STe}_4$ is composed of covalently bonded Cu–Te chains, which are interconnected via interchain, linearly coordinated S atoms forming Cu–S bonds to infinite layers. The Cu sites all have varying deficiencies, as often observed in Cu chalcogenides, and are coordinated by 3–4 chalcogen atoms in the form of distorted trigonal pyramids and tetrahedra. The multitude of short Cu–Cu contacts implies the possibility of Cu ion mobility, which in turn stands against using these chalcogenides in thermoelectric devices.

DFT-based calculations predicted these materials to be intrinsic semiconductors when $x = 0$; with the experimentally observed Cu deficiencies the materials are expected to be extrinsic (p -type) semiconductors. Electrical transport measurements performed on $\text{Ba}_2\text{Cu}_{5.5}\text{STe}_4$ and $\text{Ba}_2\text{Cu}_{5.5}\text{SeTe}_4$ confirmed this expectation.

ASSOCIATED CONTENT

Supporting Information. Four crystallographic information files (CIFs), and two DSC plots. This material is available free of charge via the Internet at <http://pubs.acs.org>.

AUTHOR INFORMATION

Corresponding Author

*E-mail: kleinke@uwaterloo.ca.

ACKNOWLEDGMENT

Financial support from the Natural Sciences and Engineering Research Council and the Canada Research Chair program (CRC for H.K.) is appreciated.

REFERENCES

- (1) Rowe, D. M. *Thermoelectrics Handbook: Macro to Nano*; CRC Press, Taylor & Francis Group: Boca Raton, FL, 2006.
- (2) Kleinke, H. *Chem. Mater.* **2010**, *22*, 604–611.
- (3) Toberer, E. S.; May, A. F.; Snyder, G. J. *Chem. Mater.* **2010**, *22*, 624–634.
- (4) Kanatzidis, M. G. *Chem. Mater.* **2010**, *22*, 648–659.
- (5) Wang, Y. C.; DiSalvo, F. J. *J. Solid State Chem.* **2001**, *156*, 44–50.
- (6) Patschke, R.; Zhang, X.; Singh, D.; Schindler, J.; Kannewurf, C. R.; Lowhorn, N.; Tritt, T.; Nolas, G. S.; Kanatzidis, M. G. *Chem. Mater.* **2001**, *13*, 613–621.
- (7) Assoud, A.; Thomas, S.; Sutherland, B.; Zhang, H.; Tritt, T. M.; Kleinke, H. *Chem. Mater.* **2006**, *18*, 3866–3872.
- (8) Cui, Y.; Assoud, A.; Xu, J.; Kleinke, H. *Inorg. Chem.* **2007**, *46*, 1215–1221.
- (9) Kuropatwa, B.; Cui, Y.; Assoud, A.; Kleinke, H. *Chem. Mater.* **2009**, *21*, 88–93.
- (10) Mayasree, O.; Cui, Y.; Assoud, A.; Kleinke, H. *Inorg. Chem.* **2010**, *49*, 6518–6524.
- (11) Debus, S.; Harbrecht, B. *Z. Anorg. Allg. Chem.* **2000**, *626*, 173–179.
- (12) Debus, S.; Harbrecht, B. *Z. Anorg. Allg. Chem.* **2001**, *627*, 431–438.
- (13) Yao, X.; Franzen, H. F. *J. Am. Chem. Soc.* **1991**, *113*, 1426–1427.
- (14) Yao, X.; Miller, G. J.; Franzen, H. F. *J. Alloys Compd.* **1992**, *183*, 7–17.
- (15) Yao, X.; Franzen, H. F. *J. Solid State Chem.* **1990**, *86*, 88–93.
- (16) Yao, X.; Franzen, H. F. *Z. Anorg. Allg. Chem.* **1991**, *598–599*, 353–362.
- (17) Yao, X.; Marking, G.; Franzen, H. F. *Ber. Bunsen Ges.* **1992**, *96*, 1552–1557.
- (18) Köckerling, M.; Franzen, H. F. *Croat. Chem. Acta* **1995**, *68*, 709–719.
- (19) Richter, K. W.; Flandorfer, H.; Franzen, H. F. *J. Solid State Chem.* **2002**, *167*, 517–524.
- (20) Kleinke, H. *Chem. Commun.* **1998**, 2219–2220.
- (21) Kleinke, H.; Franzen, H. F. *J. Am. Chem. Soc.* **1997**, *119*, 12824–12830.
- (22) Warczok, P.; Chumak, I.; Richter, K. W. *J. Solid State Chem.* **2009**, *182*, 896–904.
- (23) Kleinke, H. *Can. J. Chem.* **2001**, *79*, 1338–1343.
- (24) Kleinke, H. *J. Alloys Compd.* **2002**, *336*, 132–137.
- (25) Assoud, A.; Xu, J.; Kleinke, H. *Inorg. Chem.* **2007**, *46*, 9906–9911.
- (26) Dürichen, P.; Bolte, M.; Bensch, W. *J. Solid State Chem.* **1998**, *140*, 97–102.
- (27) Iglesias, J. E.; Pachali, K. E.; Steinfink, H. *J. Solid State Chem.* **1974**, *9*, 6–14.
- (28) Assoud, A.; Soheilnia, N.; Kleinke, H. *Chem. Mater.* **2005**, *17*, 2255–2261.
- (29) Lee, C.-S.; Kleinke, K. M.; Kleinke, H. *Solid State Sci.* **2005**, *7*, 1049–1054.
- (30) *M86-Exx078 APEX2 User Manual*; Bruker AXS Inc.: Madison, WI, 2006.
- (31) Sheldrick, G. M. *Acta Crystallogr. A* **2008**, *64*, 112–122.
- (32) Spek, A. L. *J. Appl. Crystallogr.* **2003**, *36*, 7–13.

- (33) Andersen, O. K. *Phys. Rev. B* **1975**, *12*, 3060–3083.
- (34) Skriver, H. L. *The LMTO Method*; Springer: Berlin, Germany, 1984.
- (35) Hedin, L.; Lundqvist, B. I. *J. Phys. C* **1971**, *4*, 2064–2083.
- (36) Lambrecht, W. R. L.; Andersen, O. K. *Phys. Rev. B* **1986**, *34*, 2439–2449.
- (37) Blöchl, P. E.; Jepsen, O.; Andersen, O. K. *Phys. Rev. B* **1994**, *49*, 16223–16233.
- (38) Assoud, A.; Derakhshan, S.; Soheilnia, N.; Kleinke, H. *Proc. Int. Conf. Thermoec.* **2005**, *24*, 303–310.
- (39) Pauling, L. *The Nature of the Chemical Bond*; 3rd ed.; Cornell University Press: Ithaca, NY, 1948.
- (40) Jansen, M. *Angew. Chem., Int. Ed. Engl.* **1987**, *26*, 1098–1110.
- (41) Mehrotra, P. K.; Hoffmann, R. *Inorg. Chem.* **1978**, *17*, 2187–2189.
- (42) Merz, K. M., Jr.; Hoffmann, R. *Inorg. Chem.* **1988**, *27*, 2120–2127.
- (43) Pyykkö, P. *Chem. Rev.* **1997**, *97*, 597–636.
- (44) Orlygsson, G.; Conrad, M.; Harbrecht, B. *Z. Anorg. Allg. Chem.* **2001**, *627*, 1017–1022.